

---

# Echo Cancellation

Multiple access communication, discussed in Chapter 17, usually relies on the orthogonality of the different signals by separating them in time or frequency. Analogous techniques apply to *full-duplex transmission*, or simultaneous transmission in both directions on a point-to-point link. Specifically, we can use *time-compression multiplexing (TCM)* and *frequency-division multiplexing (FDM)*. A more efficient approach, *echo cancellation* enables transmission in two directions simultaneously using the same frequency band, thereby reducing the bandwidth requirements approximately in half relative to TCM and FDM.

**Example 20-1.** Full-duplex digital transmission on a single wire pair from central office to telephone subscriber (the *digital subscriber loop*), as standardized in the United States, uses four-level baseband transmission. Given the communication engineer's penchant for obfuscation, this is called "2B1Q" line coding, which stands for "two bits on one quaternary digit". The bit rate is 160 kb/s, including 144 kb/s user data and 16 kb/s for framing and control, and the baud rate is therefore 80 kb/s. The bandwidth required on the cable is, for 0% excess bandwidth, 40 kHz. Both directions of transmission share this same bandwidth, with echo cancellation used to separate the two directions. See [1][2][3] for comparisons of the relative merits of echo cancellation and TCM in this application.

**Example 20-2.** The V.32 full-duplex modem transmits 9600 b/s in both directions over a voiceband data channel. It uses a baud rate of 2400 Hz, with four bits per symbol, and uses QAM modulation with a carrier frequency of 1800 Hz. With 0% excess bandwidth, the frequency band used would therefore be from 400 to 3000 Hz, nearly the full bandwidth of the voiceband data channel. TCM is unsuitable for voiceband data transmission because of the possibility of large propagation delays (such as on connections including a satellite link), and FDM is too bandwidth inefficient for higher speed modems.

At each end of a full-duplex link, the near-end transmitted signal can be used to eliminate the undesired interference (called an *echo*) of the near-end transmitted signal at the receiver. An *echo canceler* can learn adaptively the response from near-end transmitter to receiver, generate

a replica of that echo, and subtract that echo replica from the receiver input to yield an interference-free signal.

**Example 20-3.** In principle, echo cancellation could be used to share any medium, such as a radio channel (Section 18.4), for the two directions. A radio channel would be of great practical interest because of the limited available spectrum, but unfortunately is impractical in today's technology because of the speed, and particularly the accuracy, required for the echo cancellation. However, we cannot rule it out for the future.

## 20.1. PRINCIPLE OF THE ECHO CANCELER

When we transmit full-duplex data, the primary problem is undesired feed-through of the transmitted data signal into the receiver through the hybrid. This extraneous signal is called *echo*. The operation of the hybrid was discussed in Section 18.5, and in particular it was illustrated in Fig. 18-37, where the mechanism for echo was stated to be a mismatch between the impedance of the two-wire cable and the hybrid balancing impedance.

**Example 20-4.** As shown in Fig. 18-39, there are actually two opportunities for undesired echo on a voiceband data connection — the near-end hybrid and one or more far-end hybrids. One difficulty with the far-end echo that we will have to address is the possible frequency offset that it experiences, just as with the far-end data signal. The digital subscriber loop application is easier than the voiceband data canceler in this respect, since there is no far-end echo mechanism.

The echo cancellation method of full-duplex transmission is illustrated in Fig. 20-1. There is a transmitter (TR) and receiver (REC) on each end of the connection, and a hybrid is used to provide a virtual four-wire connection between the transmitter on each end and the receiver on the opposite end. The echo canceler is an adaptive transversal filter (Chapter 9) that adaptively learns the response of the hybrid, and generates a replica of that response which is subtracted from the hybrid output to yield an echo-free received signal.

**Example 20-5.** Typical numbers would be a 10 dB worst-case hybrid loss and 40 dB attenuation of the far-end transmitter. This implies a  $-30$  dB signal-to-echo ratio at the hybrid output, which is clearly unacceptable. This can be improved to a more reasonable  $+20$  dB by an echo canceler with an additional 50 dB echo attenuation.

The echo canceler notation is shown in Fig. 20-2. The local transmitter signal  $y(t)$  at port A generates the undesired echo signal  $r(t)$ . This signal is superimposed at the output of the hybrid (port D) with the far transmitter signal  $x(t)$ . The canceler takes advantage of its knowledge of the local transmitter signal to generate a replica of the echo,  $\hat{r}(t)$ . This replica is subtracted from the echo plus far transmitter signal to yield  $e(t)$ , which ideally contains the far transmitter signal  $x(t)$  alone. The echo canceler is usually implemented in discrete-time as a finite

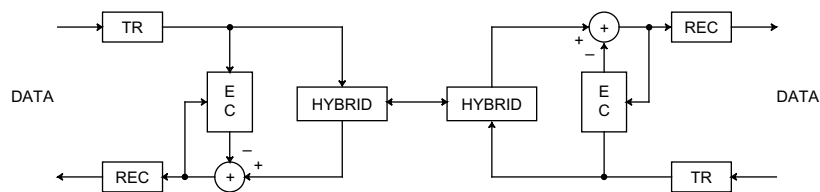


**Fig. 20-1.** Echo cancellation method of full-duplex data transmission.

transversal filter (Chapter 9) as shown in Fig. 20-3. Essentially the same stochastic gradient algorithm can be applied to adapt the canceler to the details of the echo path response as was used to adapt the equalizer.

The canceler design depends strongly on the details of the local transmitter and receiver design.

**Example 20-6.** A block diagram illustrating the functions of the digital subscriber loop transceiver is shown in Fig. 20-4 [4]. The transmit data is first scrambled (Section 19.5) to insure that there are sufficient pulses for timing recovery on the other end. Some form of line coding (Section 19.1) is applied to control the transmitted signal spectrum; for example, to insure that there is no energy at

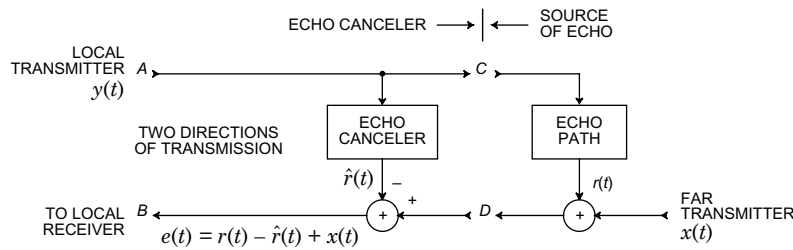


Fig. 20-2. The principle and notation of an echo canceler.

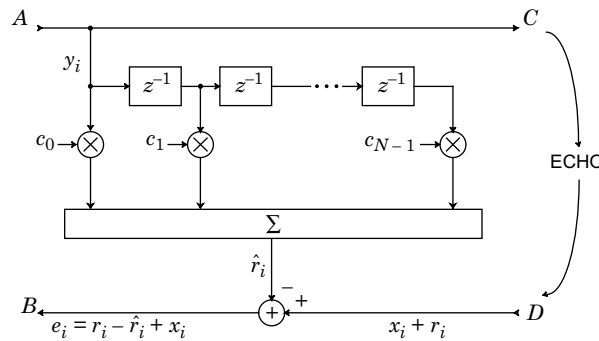


Fig. 20-3. A transversal filter echo canceler.

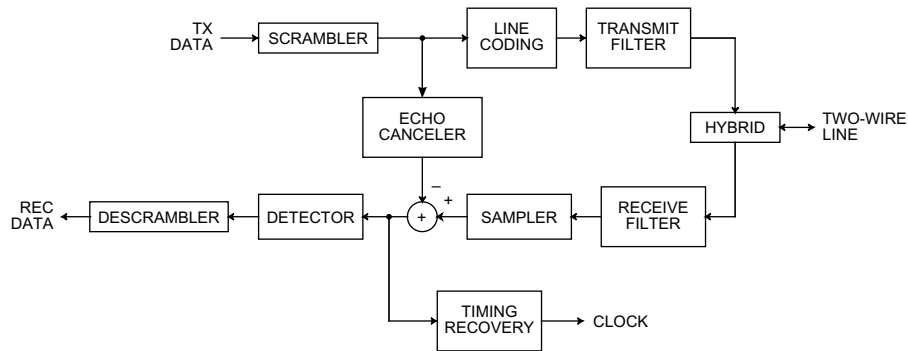


Fig. 20-4. A block diagram of a full-duplex digital subscriber loop transceiver.

d.c. Next is the transmit filter to limit the high frequency components in the signal for radio-frequency interference (RFI) and crosstalk purposes. The echo canceler is connected either before or after the line coding at a point where the echo path is linear. A receive filter prevents aliasing in the subsequent sampling operation, and may also provide equalization of the high frequency attenuation of the cable. The signal is then sampled, since the echo canceler operates in the sampled data domain. After echo cancellation, the data is detected, taking into account the line coding and any intersymbol interference present, and descrambled to yield the received data sequence. The choice of sampling rate represents a tradeoff between the complexity of the echo canceler and the ease of recovering timing. For purposes of data detection, a sampling rate equal to the data symbol rate is adequate, although there are many benefits to doubling this rate and using fractionally-spaced equalizers (Chapter 8). Timing recovery (Chapter 16) is usually considered to require a sampling rate equal to at least twice the data symbol rate (baud-rate timing recovery is also possible [5]). This implies that the echo canceler has different sampling rates at input and output, since the input sampling rate is equal to the baud rate. This is a major consideration in the echo canceler design, and is discussed in Section 20.2.

## 20.2. BASEBAND CHANNEL

There are significant differences between the baseband and passband channel echo cancelers. We defer the more complicated passband canceler to Section 20.3. Assume a transmitted PAM signal is

$$y(t) = \sum_{m=-\infty}^{\infty} a_m g(t - mT), \quad (20.1)$$

where  $a_m$  is the sequence of transmitted data symbols,  $g(t)$  is the transmitted pulse shape,  $T$  is the baud interval, and the echo has transfer function  $F(f)$ . Let  $h(t) = g(t) * f(t)$ , so the echo response is

$$r(t) = \sum_{m=-\infty}^{\infty} a_m h(t - mT). \quad (20.2)$$

Two approaches to echo cancellation are shown in Fig. 20-5a. In Fig. 20-5a we sample the transmitted data waveform  $y(t)$  at the canceler input, and in Fig. 20-5b we apply the transmitted data symbols directly to the canceler so that the transmit filter is included in the echo path. Because the transmitted and echo signals will have bandwidth greater than half the baud rate, a

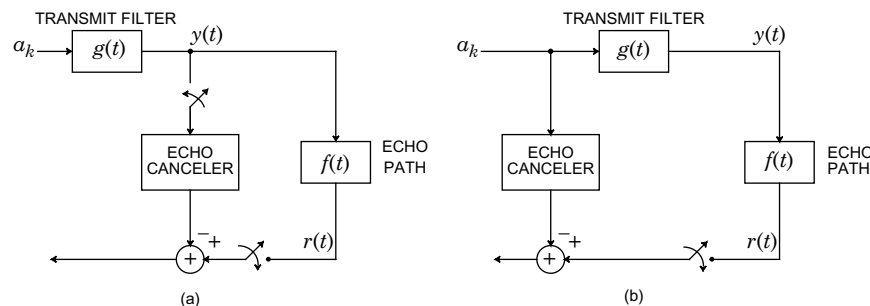


**Fig. 20-5.** Two configurations for a baseband channel echo canceler. Cancellation using a. the sampled transmitted data waveform and b. the transmitted data symbols.

sampling rate of twice the baud rate or more will be required in Fig. 20-5a. On the other hand, the sampling at the input of the canceler in Fig. 20-5b is equal to the baud rate, leading to the immediate difficulty that the sampling rate at the output of the echo canceler is higher than the sampling rate at the input! This is precisely the opposite of the situation that we encountered in the fractionally-spaced equalizer in Chapter 8, where the input sampling rate was higher than the output.

### Interleaved Echo Cancelers

There is a ready solution to the problem of incompatible sampling rate, called *interleaved echo cancelers*. Since a clock representing the transmitted data signal is available, it is natural to sample the echo signal at a rate that is an integer multiple of the transmit baud rate, say a multiple  $R$ . Define a special notation for the samples of the received signal at this rate,

$$r_k(l) = r((k + \frac{l}{R})T) , \quad 0 \leq l \leq R - 1 , \quad (20.3)$$

where the index  $k$  represents the data symbol epoch and  $l$  represents the sample from among  $R$  samples uniformly spaced in this epoch. This notation suggests an interpretation of this stream of samples as a set of  $R$  interleaved sample streams each with sampling rate equal to the baud rate. Similarly, define a notation for the samples of the echo pulse response

$$h_k(l) = h((k + \frac{l}{R})T) , \quad 0 \leq l \leq R - 1 . \quad (20.4)$$

Combining the last three equations,

$$r_k(l) = \sum_{m=-\infty}^{\infty} h_m(l) a_{k-m} . \quad (20.5)$$

This relation shows that the samples of the echo can be thought of as  $R$  independent echo channels, each channel being driven by an identical sequence of data symbols. The discrete-time impulse response of the  $l$ -th echo channel is  $h_k(l)$ .

The echo replica can be generated independently for each echo channel by a set of  $R$  *interleaved echo cancelers* as shown in Fig. 20-6. Each canceler cancels the echo for one sampling phase, from among  $R$ , and has a sampling rate at the input and output equal to the baud rate. Each canceler operates independently of the other; in particular, each generates its own error signal for purposes of both the full-duplex data receiver and the adaptation of the corresponding canceler.

Since the  $R$  echo channels are independent, the index  $l$  can be dropped. In the sequel we need only consider the design of one of the interleaved echo cancelers, and all the others follow naturally. The transversal filter echo canceler generates the replica

$$\hat{r}_k = \sum_{m=0}^{N-1} c_m a_{k-m} , \quad (20.6)$$

where  $\{c_0, \dots, c_{N-1}\}$ , are the  $N$  filter coefficients of one of the  $R$  interleaved transversal filters. This transversal filter generates an FIR approximation to the echo response  $h_m(l)$ .

Each canceler can be thought of as adapting to the impulse response of the echo channel sampled at a rate equal to the baud rate, but with a particular phase out of  $R$  possible phases. These cancelers independently converge, although they do have in common the same input

sequence of data symbols. Since the transversal filters all adapt independently, the presence of multiple interleaved canceler filters does not affect the speed of adaptation. Therefore, the choice of an output sampling rate is purely a question of implementation complexity; the adaptation rate and asymptotic error are not affected by the sampling rate.

Returning to Fig. 20-5, the interleaved canceler required in Fig. 20-5b has important advantages over the configuration of Fig. 20-5a [6]:

- The input to the canceler is transmitted data symbols, with a finite (and usually small) alphabet. The implementation of the canceler therefore requires a relatively simple multiplier, since the transmitted data symbols have a very few bits (perhaps as low as one) of precision.
- The speed of adaptation is greater, since the interleaved cancelers adapt independently and each has fewer taps.
- The canceler complexity as measured by the multiplication rate is lower, as illustrated by the following example.

**Example 20-7.** If the sampling rate for the received signal is  $R$  samples per baud, and the effective length of the echo impulse response is  $N$  baud intervals (which we assume is not affected appreciably by the presence of the transmit filter in the echo response path), we can compare the multiplication rate for Fig. 20-5a and b. In Fig. 20-5a the convolution sum will have  $NR$  taps, each of which must be calculated  $R$  times per baud, for a total multiplication rate equal to  $NR^2$  times the baud rate. In Fig. 20-5b each of the interleaved cancelers will have  $N$  taps, calculated at the baud rate, for a multiplication rate equal to  $N$  times the baud rate. Considering that there are  $R$  interleaved

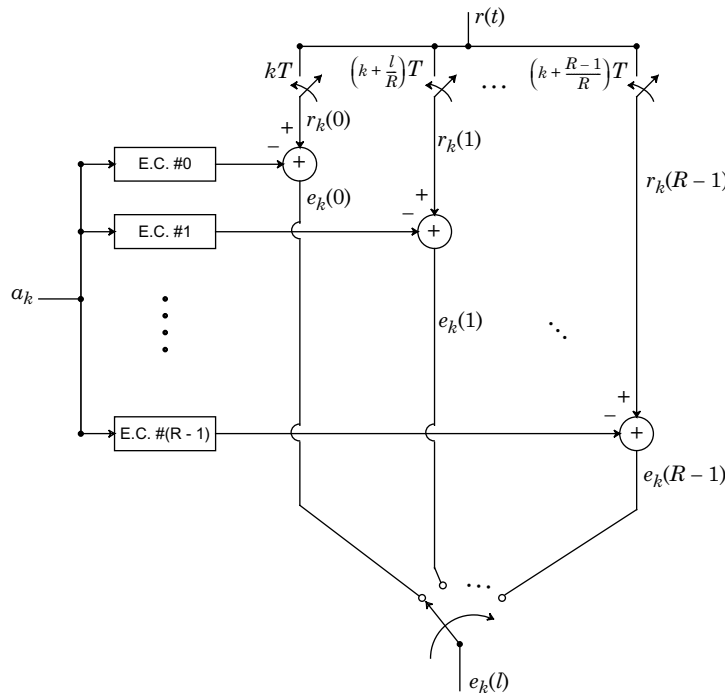


**Fig. 20-6.** A set of  $R$  interleaved echo cancelers, each canceling one of  $R$  phases.

cancelers, the total multiplication rate is  $NR$  times the baud rate. The interleaved canceler therefore has a multiplication rate lower by a factor of  $R$ .

For all these reasons, the configuration of Fig. 20-5b is generally preferred over Fig. 20-5a.

### 20.3. PASSBAND CHANNEL

The *passband echo canceler* is considerably different from the baseband channel case. Assuming the data symbols are applied directly to the canceler as in Fig. 20-5b, there are two obvious differences:

- The canceler input is complex-valued.
- The transmitter modulator is included in the transmit path, so that the echo path is *time-varying*. An adaptive filter could in principle model track this time varying channel, but in practice the required adaptation speed could not be achieved.

Fortunately, the carrier frequency and phase is precisely known, so that we can compensate for the carrier by adding a similar modulator to the transversal filter. There are numerous configurations possible, as we will see in this section. Pioneering work on the passband channel canceler was done by S. Weinstein of Bell Laboratories [7]. We begin by developing a model for the echo path.

#### 20.3.1. Echo Path Model

A model for the transmitter and echo path is shown in Fig. 20-7a. The transmit filter is  $g(t)$  and the echo path impulse response is  $f(t)$ . For the time being we assume that a phase splitter is included in the receive circuitry to generate the analytic signal, although we will see alternative configurations. The equivalent model shown in Fig. 20-7b follows directly from the results of Chapter 5, since transmitting a passband PAM signal through a communication channel is no different from transmitting through an echo channel. The received echo signal is

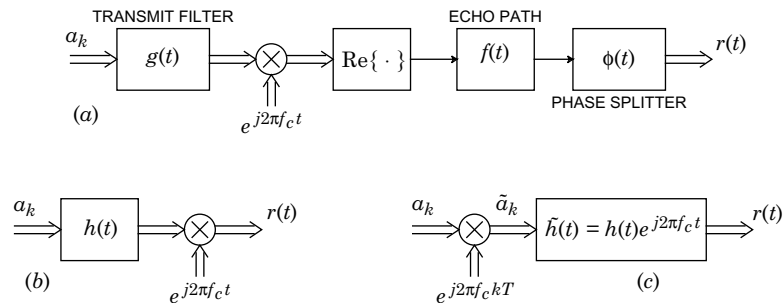


**Fig. 20-7.** The transmitter and echo path for a passband channel echo canceler. a. The transmitter, echo path, and a phase splitter at the receiver input. b. An equivalent model for the path from transmitted data symbols to received analytic signal consisting of a baseband echo channel followed by modulator. c. An alternative model consisting of a modulator followed by passband echo channel.

$$r(t) = \sqrt{2} \operatorname{Re} \left\{ \sum_{k=-\infty}^{\infty} \alpha_k h(t - kT) e^{j2\pi f_c t} \right\}, \quad (20.7)$$

where the equivalent baseband complex-valued response is (see Section 2.4),

$$h(t) = (f(t) e^{-j2\pi f_c t}) * g(t), \quad H(f) = F(f + f_c) G(f). \quad (20.8)$$

The conclusion is that the echo channel output can be considered as a signal of the same form as the transmitted signal, except the transmitted baseband pulse  $g(t)$  has been replaced by an echo-channel equivalent baseband output pulse  $h(t)$ . The latter is obtained by shifting the echo transfer function in the vicinity of the carrier frequency down to d.c. Since  $h(t)$  is in general complex-valued, even though the transmit pulse  $g(t)$  is real-valued, the echo canceler must have complex-valued tap coefficients! This of course implies that there is crosstalk between the in-phase and quadrature channels when they pass through the echo channel, similarly to the situation in channel equalization.

After a minor manipulation, the analytic signal corresponding to (20.7) at the output of a phase splitter can be written in the form

$$r(t) = \sum_k \alpha_k e^{j2\pi f_c kT} h(t - kT) e^{j2\pi f_c (t - kT)} = \sum_k \tilde{\alpha}_k \tilde{h}(t - kT) \quad (20.9)$$

where

$$\tilde{h}(t) = h(t) e^{j2\pi f_c t} \quad (20.10)$$

is an equivalent passband pulse waveform and

$$\tilde{\alpha}_k = \alpha_k e^{j2\pi f_c kT} \quad (20.11)$$

is called the *rotated data symbol* since it is simply rotated by angle  $2\pi f_c kT$  radians. This results in the model of Fig. 20-7c. The rotation of the data symbols is in effect a modulation up to passband, and then the rotated symbols are put through an equivalent passband channel with impulse response  $\tilde{h}(t)$ . Since  $h(t)$  is a baseband pulse, this filter has a response centered at the carrier frequency. The rotation of the data symbols is simple to implement when the carrier frequency and baud rate have a simple relationship.

**Example 20-8.** For a V.32 modem, the carrier frequency is 1800 Hz and the baud rate is 2400 Hz. Therefore,

$$2\pi f_c T = 2\pi \frac{1800}{2400} = \frac{3\pi}{2} \text{ radians.} \quad (20.12)$$

For this case, the exponent  $2\pi f_c kT$  assumes only multiples of  $\pi/2$ , and hence the rotation requires only multiplication by values that are of the form  $\pm 1$  or  $\pm j$ . The rotation in this case is always by some multiple of 90 degrees.

### 20.3.2. Interleaved Passband Channel Echo Cancelers

Just as in the baseband case, the sampling rate at the receiver input will generally be a multiple  $R$  of the baud rate, necessitating interleaved echo cancelers. Defining  $r_i(l)$ ,  $h_i(l)$ , and  $\tilde{h}_i(l)$  as in (20.3) and (20.4), a relation similar to (20.5) is obtained. For the echo channel model of Fig. 20-7b, we get

$$r_k(l) = \left[ \sum_m a_m h_{k-m}(l) \right] e^{j2\pi f_c(k+l/R)T}, \quad (20.13)$$

and for the echo channel model of Fig. 20-7c we get

$$r_k(l) = \sum_m \tilde{a}_m \tilde{h}_{k-m}(l) . \quad (20.14)$$

In both cases we can implement the canceler as  $R$  independent interleaved cancelers.

### 20.3.3. Passband vs. Baseband Transversal Filters

Based on the discrete-time interleaved representations for the echo channel represented by (20.13) and (20.14), there are two echo canceler configurations to synthesize these echo responses as pictured in Fig. 20-8. The difference between these two configurations is the placement of the modulator after or before the complex-coefficient transversal filter.

The baseband transversal filter of Fig. 20-8a follows directly from the representation of Fig. 20-7b and (20.13). Let the transversal filter have  $N$  complex-valued coefficients  $\{c_0, \dots, c_{N-1}\}$ , in which case the echo canceler can be represented mathematically as

$$\hat{r}_k(l) = \left[ \sum_{m=0}^{N-1} c_m a_{k-m} \right] e^{j2\pi f_c(k+l/R)T} . \quad (20.15)$$

This can be represented as a transversal filter, which performs the convolution sum, followed by a modulator. The transversal filter is approximating the equivalent baseband pulse  $h(t)$  in the model of Fig. 20-7b, and hence we call it a *baseband transversal filter*.

An equivalent configuration follows from the model of Fig. 20-7c and (20.14), from which we get an echo canceler of the form

$$\hat{r}_k(l) = \sum_{m=0}^{N-1} c_m \tilde{a}_{k-m} . \quad (20.16)$$

This configuration is shown in Fig. 20-8b. The rotator first modulates the data symbols to passband, and the transversal filter then approximates the passband response  $\tilde{h}(t) = h(t)e^{j2\pi f_c t}$ . For this reason we call this a *passband transversal filter*.

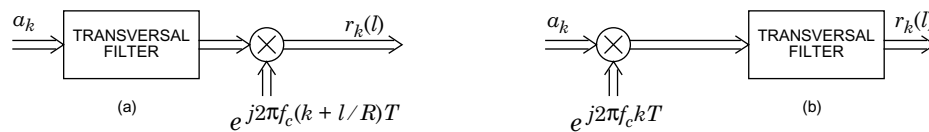


**Fig. 20-8.** Two configurations for one interleaved echo canceler corresponding to a passband channel. a. A baseband transversal filter followed by modulator. b. A modulator followed by a passband transversal filter.

### 20.3.4. Real vs. Complex Error Cancelers

Yet another option in cancelers for a passband channel is the generation of a real-valued or complex-valued error signal as illustrated in Fig. 20-9. The complex-error configuration of Fig. 20-9a is the one considered thus far in this section. It is assumed that the receive analytic signal is generated using a phase splitter, and the echo canceler generates a replica of the echo analytic signal.

The real-error alternative shown in Fig. 20-9b cancels only the real part of the analytic signal, which in actuality is the passband receive waveform. For this case, only the real part of the canceler complex-valued output is required. Use of the real-error canceler can reduce the canceler computational load because only the real part of the output need be calculated. Similarly, the receive signal is used in place of the analytic signal, the former being the real part of the latter, thereby eliminating the need for the phase splitter. Overall, then, the complexity of the real-error canceler is lower.

We will see in the next section that the convergence of the complex-error canceler is faster than that of the real-error canceler, because the former makes use of more information. Further, in some circumstances the savings of a phase splitter in a real-error canceler is negated by the need for a splitter in the data receiver that follows the echo canceler. On the other hand, the real-error canceler is especially attractive in the Nyquist cancellation application described in the next subsection.

### 20.3.5. Nyquist Cancellation

In voiceband data modems, the two directions of transmission are governed by independent clocks, and therefore there will be a frequency offset. This implies that the sampling clock used for echo cancellation is not necessarily the same in frequency or phase as the appropriate sampling clock for recovery of the far-end data. The usual solution to this problem is to use a *Nyquist canceler* which operates at a sufficiently high sampling rate to allow recovery of a continuous-time version of the far-end data signal. This far-end signal can then be resampled in accordance with the appropriate clock without regard to its phase or frequency relative to the transmit data clock.

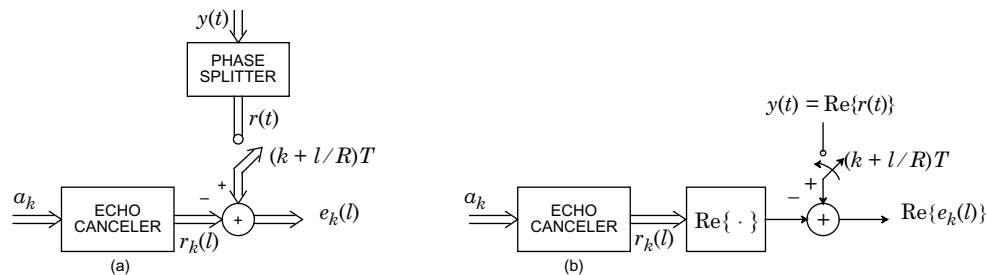


**Fig. 20-9.** Two options for passband channel echo cancellation (shown is one of  $R$  interleaved cancelers). a. Complex-error canceler, requiring phase splitter before cancellation. b. Real-error canceler, requiring no phase splitter.

The Nyquist canceler is shown in Fig. 20-10. The canceler works on samples generated synchronously with the transmit data stream (the dashed line indicates the source of the clock for each sampler). The bandpass filter (BPF) prior to the sampler eliminates all noise out-of-band of the received data signal (and incidently some of the echo as well). The sampling rate is chosen to be Nyquist; that is, greater than twice the highest frequency in the receive data signal. For convenience it will be an integral multiple of the transmit baud rate clock.

After recovery of the receive data signal without the echo, a continuous-time receive signal is recovered using a lowpass filter (LPF). This signal is then resampled synchronously with the receive data signal using a clock provided by the receiver.

An advantage of the Nyquist canceler is that an existing half-duplex data receiver can be used without modification. The purpose of the echo cancellation “front-end” is merely to eliminate the undesired echo interference from the transmitter. Note also that a real-error canceler has been used and is attractive in this configuration, since there is a savings of a phase splitter. Only one phase splitter is required, the one in the receiver.

## 20.4. ADAPTATION

As with adaptive equalizers (Chapter 9), there are two measures of performance of an adaptive echo canceler: the speed of adaptation and the accuracy of the cancellation after adaptation. There is a tradeoff between these two measures: for a particular class of adaptation algorithm, as the speed of adaptation is increased the accuracy of the transfer function after adaptation gets poorer. This tradeoff is fundamental, since a longer averaging time is necessary to increase asymptotic accuracy, but slows the rate of convergence. Usually the motivation for adapting an echo canceler is that the transfer function of the echo is not known in advance. It is also probable that the echo transfer function is changing with time, although in most cases the change will be quite slow (say in response to changes in the temperature of the transmission facilities). Thus, in most instances the accuracy of the final cancellation of the echo is the most critical design factor.

**Example 20-9.** In the digital subscriber loop, the transceiver will often be dedicated to a particular loop. As long as the transceiver is allowed to run all the time, or at least stores the echo canceler coefficients between calls, the adaptation can be quite slow (resulting in a high accuracy) because

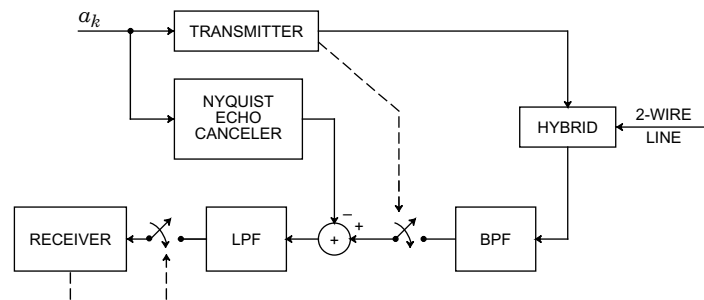


**Fig. 20-10.** A Nyquist echo canceler operating synchronously with the transmitted data stream and asynchronously from the data receiver.

the echo path transfer function should change only in response to temperative changes and similar influences, which occur quite slowly.

Although the ability of the canceler to rapidly track a changing echo response is usually not important, the speed of initial adaptation from an arbitrary initial condition is often important.

**Example 20-10.** In a voiceband data modem, the echo canceler must converge anew at the beginning of each call. The adaptation of the echo canceler is therefore a part of the initialization sequence before useful data transmission can occur. Since one would like to minimize that initialization time, there is motivation to adapt as quickly as possible. This is a natural application for a gear-shifting algorithm, since the accuracy of cancellation is not critical during the training period (no actual data transmission is taking place) and therefore it is permissible to start with a larger step-size. With respect to the the far-end echo canceler (Section 20.6) a more rapid tracking capability will be required.

We will derive a SG adaptation algorithm for the complex-error passband transversal filter algorithm in this section [8]. The case of a baseband channel canceler is a special case [9][10][11] and will also be covered. The adaptation of the baseband transversal filter canceler for the passband channel is a simple extension and is relegated to the problems [7]. The adaptation of the real-error canceler is a bit more complicated to derive and analyze and is relegated to Appendix 20-A. More general results on adaptation algorithms and their convergence can be found in [12].

As usual, we consider the minimum MSE problem first, followed by the SG algorithm. In all cases we will derive the adaptation algorithm for only one of the  $R$  interleaved cancelers, and assume that same algorithm is applied identically to all.

### 20.4.1. Minimum MSE Solution

In this section we consider the optimum tap coefficients for a complex-error passband transversal filter canceler. Write the  $m$ -th filter coefficient as  $c_m$  and the analytic echo cancellation error at time  $k$  as  $E_k$ . Define a notation for the vector of  $N$  filter coefficients

$$\mathbf{c} = [c_0, c_1, \dots, c_{N-1}]'. \quad (20.17)$$

For the passband transversal filter canceler, the input to the transversal filter is the rotated data symbol  $\tilde{A}_k$ . Define a vector of the current and  $N-1$  past input rotated data symbols

$$\tilde{\mathbf{a}}_k = [\tilde{A}_k, \tilde{A}_{k-1}, \dots, \tilde{A}_{k-N+1}]. \quad (20.18)$$

If the impulse response of the echo channel is  $\tilde{h}_k(l)$ ,  $0 \leq k < \infty$  for the  $l$ -th interleaved canceler, then it is also convenient to define a vector of the first  $N$  of these impulse response samples,

$$\tilde{\mathbf{h}} = [\tilde{h}_0, \tilde{h}_1, \dots, \tilde{h}_{N-1}]', \quad (20.19)$$

where in this and subsequent equations the “ $l$ ” is suppressed. All of these quantities are complex-valued, except in the baseband channel case where they are real-valued.

With this notation in hand, the analytic error signal can be written as

$$E_k = \sum_{m=0}^{\infty} \tilde{h}_m \tilde{A}_{k-m} - \sum_{m=0}^{N-1} c_m \tilde{A}_{k-m} + X_k$$

$$= (\tilde{\mathbf{h}} - \mathbf{c})' \tilde{\mathbf{a}}_k + V_k, \quad (20.20)$$

where  $X_k$  is the far-end data signal plus noise and

$$V_k = \sum_{m=N}^{\infty} \tilde{h}_m \tilde{A}_{k-m} + X_k \quad (20.21)$$

is the residual uncancelable echo. This uncancelable echo has several components:

- Echo components with delays that exceed the number of coefficients in the transversal filter,
- The noise introduced on the channel from the far-end data transmitter, and
- The far-end data signal, which represents a noise with respect to the adaptation of the echo canceler.

For the MSE solution, we assume that  $\tilde{A}_k$  is a wide-sense stationary discrete-time random process and that the echo channel  $\tilde{h}_k$  is known. We want to minimize the MSE error  $E(|E_k|^2)$ . This error signal includes, as one component, the far-end data signal, which we don't wish to minimize. Fortunately, the echo canceler has no influence over this data signal. As long as the data signals in the two directions are uncorrelated, minimizing the MSE will be the same as minimizing the component of echo in the error signal (as we will see).

Following consistent notation to Section 9.2, define

$$\mathbf{p} = E[V_k \tilde{\mathbf{a}}_k], \quad \Phi = E[\tilde{\mathbf{a}}_k^* \tilde{\mathbf{a}}_k'] , \quad (20.22)$$

where these quantities are independent of  $k$  due to the wide-sense stationarity assumption. The autocorrelation of the rotated data symbols is easily related to the autocorrelation of the data symbols itself.

**Exercise 20-1.** Show that the relationship between the rotated and non-rotated data symbol autocorrelation functions is,

$$E[\tilde{A}_k \tilde{A}_k^*] = e^{j2\pi f_c(k-m)T} E[A_k A_m^*] . \quad (20.23)$$

This demonstrates that if the data symbols are wide-sense stationary, then so too are the rotated symbols, where the relationship between the power spectra is

$$S_{\tilde{a}}(e^{j2\pi fT}) = S_a(e^{j2\pi(f-f_c)T}). \quad (20.24)$$

A simplification of the analysis of the echo canceler relative to the adaptive equalizer is that we can generally assume that the successive input data symbols are uncorrelated. This implies that the power spectrum is white, and from (20.24) the rotated data symbols are white also. In addition, since  $|\tilde{A}| = |A_k|$  the rotated symbols have the same variance as the symbols themselves. It follows for this case that the autocorrelation matrix  $\Phi$  is diagonal,

$$\Phi = \sigma_a^2 \mathbf{I}, \quad \sigma_a^2 = E[|A_k|^2] . \quad (20.25)$$

Explicitly evaluating the mean-square error,

$$E[|E_k|^2] = (\tilde{\mathbf{h}} - \mathbf{c})^* \Phi (\tilde{\mathbf{h}} - \mathbf{c}) - 2\text{Re}\{(\tilde{\mathbf{h}} - \mathbf{c})^* \mathbf{p}\} + \sigma_v^2 , \quad (20.26)$$

where  $\sigma_v^2 = E[|V_k|^2]$  is the variance of the uncancelable echo. This is a Hermitian form in the tap weight vector  $\mathbf{c}$ , and hence there is a unique minimum. (20.26) can be written in the form

$$E[|E_k|^2] = \xi_{\min} + (\mathbf{c} - \mathbf{c}_{\text{opt}})^* \Phi (\mathbf{c} - \mathbf{c}_{\text{opt}}) \quad (20.27)$$

where

$$\mathbf{c}_{\text{opt}} = \tilde{\mathbf{h}} + \Phi^{-1} \mathbf{p}, \quad \xi_{\min} = \sigma_v^2 - \mathbf{p}^* \Phi^{-1} \mathbf{p}. \quad (20.28)$$

**Example 20-11.** For the autocorrelation of (20.25), this solution reduces to

$$\mathbf{c}_{\text{opt}} = \tilde{\mathbf{h}} + \frac{1}{\sigma_a^2} \mathbf{p}, \quad \xi_{\min} = \sigma_v^2 - \frac{1}{\sigma_a^2} \|\mathbf{p}\|^2. \quad (20.29)$$

The  $\Phi$  matrix is Hermitian and non-negative definite, and has non-negative real-valued eigenvalues.

For the optimal solution to be unique, we have to assume  $\Phi$  is positive-definite, implying it is invertible, in which case this inverse  $\Phi^{-1}$  is also a Hermitian matrix. In this event, the second term in (20.27) is non-negative and has a unique minimum  $\mathbf{c} = \mathbf{c}_{\text{opt}}$ . This choice also minimizes the mean-square error, with resultant minimum value  $E[|E_k|^2] = \xi_{\min}$ .

**Example 20-12.** If the data symbols are uncorrelated with the uncancelable error, or  $\mathbf{p} = \mathbf{0}$ , then the optimum tap weight vector is equal to the echo impulse response  $\mathbf{c}_{\text{opt}} = \tilde{\mathbf{h}}$  and the resultant mean-square error is equal to the variance of the uncancelable echo,  $\xi_{\min} = \sigma_v^2$ . The optimum coefficient vector and resulting MSE are independent of the autocorrelation matrix  $\Phi$ . This condition will hold when the far-end data signal  $X_k$  is uncorrelated with the near-end data symbols. When that condition is violated, the optimum coefficient vector is not equal to the echo impulse response. This imposes a system requirement for proper operation that the data symbols in the two directions be uncorrelated. If this is violated, the echo cancellation adaptation will be biased away from replicating the echo impulse response.

## 20.4.2. Stochastic Gradient (SG) Algorithm

As with adaptive equalization, the most widely used adaptation algorithm for the echo canceler is the stochastic gradient (SG) algorithm. This is very similar to the algorithm we derived for adaptive equalizers in Chapter 9.

Consider the passband transversal filter case. The first step is to determine the magnitude-squared of the analytic cancellation error as a function of the coefficient vector  $\mathbf{c}$ ,

$$|E_k|^2 = |R_k - \mathbf{c}' \tilde{\mathbf{a}}_k|^2 = |R_k|^2 - 2\text{Re}\{\mathbf{c}^* R_k \tilde{\mathbf{a}}_k^*\} + \mathbf{c}^* \tilde{\mathbf{a}}_k^* \tilde{\mathbf{a}}_k' \mathbf{c} \quad (20.30)$$

and then we take the gradient of this expression with respect to  $\mathbf{c}$ . In view of Exercise 9-5 and the fact that the matrix  $\tilde{\mathbf{a}}_k^* \tilde{\mathbf{a}}_k'$  is Hermitian, we get

$$\nabla_{\mathbf{c}} |E_k|^2 = 2 \tilde{\mathbf{a}}_k^* \tilde{\mathbf{a}}_k' \mathbf{c} - 2R_k \tilde{\mathbf{a}}_k^* = -2E_k \tilde{\mathbf{a}}_k^* \quad (20.31)$$

The SG algorithm follows from evaluating this gradient at the last coefficient vector, multiplying by step-size  $\beta/2$ , and subtracting the result from the last coefficient vector to get the new coefficient vector,

$$\mathbf{c}_k = \mathbf{c}_{k-1} + \beta E_k \tilde{\mathbf{a}}_k^* , \quad (20.32)$$

$$E_k = R_k - \mathbf{c}'_{k-1} \tilde{\mathbf{a}}_k . \quad (20.33)$$

The implementation of this algorithm is very similar to the adaptive equalizer case of Chapter 9, with one important difference; namely, the input samples  $\tilde{A}_k$  are the rotated transmit data symbols, and are typically drawn from a relatively small alphabet. This can simplify the implementation of the multiplications in both the convolution sum and the adaptation algorithm. The baseband channel case follows as a special case, where all quantities are real-valued and  $f_c = 0$ . The derivation of SG adaptation algorithms for other canceler structures of interest is relegated to exercises.

**Exercise 20-2.** Show that the stochastic gradient adaptation algorithm for the complex-error canceler with baseband transversal filter is

$$\mathbf{c}_k = \mathbf{c}_{k-1} + \beta e^{j2\pi f_c(k+1/R)T} E_k \mathbf{a}_k^* \quad (20.34)$$

$$E_k = R_k - e^{j2\pi f_c(k+1/R)T} \mathbf{c}'_{k-1} \mathbf{a}_k . \quad (20.35)$$

*Hint:* See the hint for Problem 20-6.

**Exercise 20-3.** Show that the stochastic gradient adaptation algorithm for the real-error canceler with passband transversal filter is

$$\mathbf{c}_k = \mathbf{c}_{k-1} + \beta \text{Re}\{E_k\} \mathbf{a}_k^* , \quad (20.36)$$

$$\text{Re}\{E_k\} = \text{Re}\{R_k\} - \text{Re}\{\mathbf{c}'_{k-1} \mathbf{a}_k\} . \quad (20.37)$$

In the remainder of this section we will consider the convergence properties of the adaptation algorithm. Since the convergence analysis is so similar to the adaptive equalization case of Chapter 9, we can draw many results from there.

### 20.4.3. Convergence of the SG Algorithm

Defining a coefficient error vector

$$\mathbf{q}_k = \mathbf{c}_k - \mathbf{c}_{\text{opt}} , \quad (20.38)$$

the first step is to derive a stochastic difference equation for this error vector.

**Exercise 20-4.** Define a stochastic matrix

$$\Gamma_k = \mathbf{I} - \beta \tilde{\mathbf{a}}_k^* \tilde{\mathbf{a}}_k' \quad (20.39)$$

and define the error of the optimal fixed coefficient echo canceler,

$$D_k = R_k - \mathbf{c}'_{\text{opt}} \tilde{\mathbf{a}}_k . \quad (20.40)$$

Then show that the coefficient error vector is governed by the stochastic difference equation

$$\mathbf{q}_k = \Gamma_k \mathbf{q}_{k-1} + \beta D_k \mathbf{a}_k^* . \quad (20.41)$$

We can also determine the excess MSE of the canceler directly from (20.27),

$$E[|E_k|^2] = \xi_{\min} + E[\mathbf{q}_k^{*'} \Phi \mathbf{q}_k] . \quad (20.42)$$

These results are identical to the stochastic difference equation derived for the adaptive equalizer of Chapter 9, with minor changes in notation reflecting the different application, and so we can use the results derived there directly in analyzing the echo canceler.

In particular, for the case of uncorrelated data symbols of (20.25), (20.42) becomes

$$E[|E_k|^2] = \xi_{\min} + \sigma_a^2 E[\|\mathbf{q}_k\|^2] , \quad (20.43)$$

where the expected vector norm approximately obeys the difference equation

$$E[\|\mathbf{q}_{k+1}\|^2] = \gamma \cdot E[\|\mathbf{q}_k\|^2] + \beta^2 \sigma_a^2 \xi_{\min} , \quad (20.44)$$

$$\gamma = 1 - 2\beta\sigma_a^2 + \beta^2 N \sigma_a^4 . \quad (20.45)$$

The time constant of convergence of MSE can be obtained from setting  $\gamma^\tau = 1/e$ , from which we get

$$\tau \approx \frac{1}{2\beta\sigma_a^2} . \quad (20.46)$$

The maximum convergence rate for excess MSE is reached at

$$\beta_{opt} = \frac{1}{N\sigma_a^2} , \quad (20.47)$$

with a resulting time constant

$$\tau \approx N/2 . \quad (20.48)$$

The asymptotic excess MSE from (20.44) is

$$E[\|\mathbf{q}_k\|^2] \rightarrow \frac{N\beta}{2 - N\beta\sigma_a^2} \xi_{\min} , \quad (20.49)$$

and at the optimum step-size (optimum in terms of rate of convergence of MSE, not the asymptotic MSE), the asymptotic error is

$$E[\|\mathbf{q}_k\|^2] \rightarrow \frac{1}{\sigma_a^2} \xi_{\min} . \quad (20.50)$$

In view of (9.66), the asymptotic MSE is

$$E[|E_k|^2] \rightarrow \xi_{\min} + \xi_{\min} = 2\xi_{\min} . \quad (20.51)$$

Thus, for the fastest convergence, the total MSE is twice the minimum MSE for a fixed coefficient filter, with half that MSE attributable to the asymptotic wandering of the filter coefficients about their optimum value.

**Example 20-13.** Continuing Example 20-12, since  $\xi_{\min}$  is the variance of the uncanceled error for this case, the asymptotic MSE is for this case

$$E[|E_k|^2] \rightarrow 2\sigma_v^2 . \quad (20.52)$$

Since (hopefully) the dominant component of the uncancellable error is the far-end data signal, this implies that for the choice of the optimum step-size the SNR, defined as the ratio of the far-end data signal power to excess MSE for cancellation, will be 0 dB. In words, the residual echo will have the same power as the received signal. This is, of course, not practical, so a smaller step-size resulting in slower convergence will be required.

The analysis of convergence applies equally well to the baseband channel case, virtually without modification. The baseband transversal filter canceler analysis is also straightforward based on the results so far (Problem 20-7). The real-error canceler is a bit more complicated, and hence is relegated to Appendix 20-A. The results there can be summarized succinctly as follows. For the same step-size, the real-error canceler converges with a time constant that is approximately twice as great as the complex-error canceler. In retrospect, this is not surprising since the real-error canceler is in effect throwing away half the information available (the imaginary part of the analytic error). Both cancelers have approximately the same asymptotic MSE. Thus, we must trade off the (in some circumstances) simpler implementation of the real-error canceler against its poorer convergence properties.

## 20.5. FAR-END ECHO

In the voiceband data modem, echo can occur not only at the near-end in conjunction with the four-wire to two-wire converter, but also at intermediate points in the telephone network. These echos are generally more attenuated than the near-end echo, and hence require a less accurate cancellation, but they are also subject to additional impairments such as jitter and frequency offset. Hence, very accurate cancellation of these echos requires the addition of algorithms to the basic echo canceler considered thus far.

As always, the structure of the echo canceler depends on the assumed model for the far-end echo mechanism. One such model is shown in Fig. 20-11. We have added to the usual passband filter operating on the rotated symbols two additional features:

- A *bulk delay* accounting for the propagation delay from the transmitter to the point of echo generation.
- A carrier phase rotation by angle  $\theta(t)$  at the output to account for possible phase jitter and frequency offset in the echo channel (frequency offset would of course result in a linearly increasing phase component).

A possible configuration for a voiceband data modem echo canceler based on this model is shown in Fig. 20-12. We have shown the passband transversal filter with complex-error for convenience. The near-end echo canceler is identical to that considered earlier in this chapter — we do not expect to experience phase jitter or frequency offset in this echo path since the primary source of this echo is the hybrid within the voiceband data modem itself. The far-end

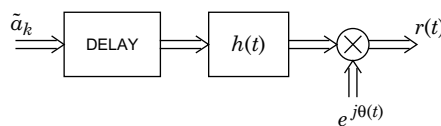


Fig. 20-11. Model of far-end echo generation mechanism.

echo canceler, however, replicates the model of Fig. 20-11. It consists of a bulk delay, which hopefully matches the delay of the echo channel, a passband transversal filter, and a phase rotator by angle  $\hat{\theta}_k$  which hopefully matches the carrier phase rotation  $\theta_k$  of the echo channel. The appropriate angle for rotation is determined by a phase-locked loop, which uses the transversal filter output and cancellation error to correct the currently used phase in a similar manner to the carrier recovery circuitry discussed in Chapter 15.

The model of Fig. 20-11 and hence the structure of Fig. 20-12 may be oversimplified. For example, the actual channel may have filtering before and after the phase rotation, rather than just before as shown in Fig. 20-11. Such a situation will require a correspondingly more complicated echo canceler structure.

A PLL algorithm can be derived using a stochastic gradient (SG) approach, in which we take the derivative of  $|E_k|^2$  with respect to the PLL output phase  $\hat{\theta}_k$ .

**Exercise 20-5.** Show that for error

$$E_k = R_k - e^{j\hat{\theta}} \mathbf{c}'_k \tilde{\mathbf{a}}_k, \quad (20.53)$$

the derivative of the MSE with respect to  $\hat{\theta}$  is

$$\frac{\partial |E_k|^2}{\partial \hat{\theta}} = -2\text{Im}\{e^{-j\hat{\theta}} E_k \mathbf{c}'_k \tilde{\mathbf{a}}_k\}. \quad (20.54)$$

By adjusting  $\hat{\theta}_k$  in the opposite direction of this derivative, we can track the phase error. The result in (20.54) has a simple and intuitive interpretation shown in Fig. 20-13. As shown in Fig. 20-13a, the goal is for the echo replica  $e^{j\hat{\theta}} \mathbf{c}'_k \tilde{\mathbf{a}}_k$  to equal the echo signal  $R_k$ , or to have the error signal  $E_k$  equal to zero. The diagram assumes that there is no far-end data signal or noise ( $R_k$  consists only of echo) and that the echo canceler transversal filter has converged so that the only difference between  $R_k$  and the echo replica is a phase rotation by  $\theta_k - \hat{\theta}$ . Under these assumptions, the actual echo is  $\mathbf{c}'_k \tilde{\mathbf{a}}_k$  rotated by  $\theta_k$ , and the echo replica is  $\mathbf{c}'_k \tilde{\mathbf{a}}_k$  rotated by  $\hat{\theta}$ .

Now, multiplying  $E_k$  by  $e^{-j\hat{\theta}} \mathbf{c}'_k \tilde{\mathbf{a}}_k$  is equivalent to rotating the entire constellation by  $-\gamma$ , where  $\gamma$  is the angle of the echo replica relative to the real-axis. This rotation places the echo replica on the real-axis as shown in Fig. 20-13b. In this rotated constellation it is easy to tell

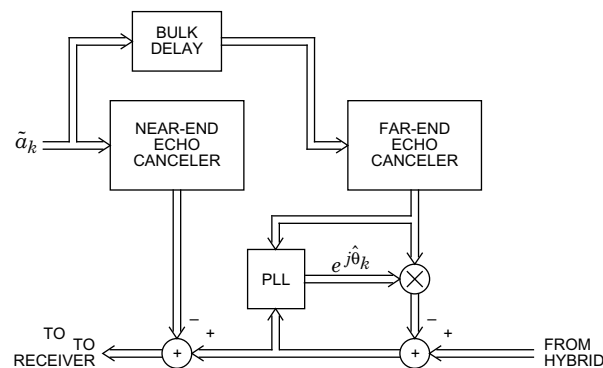


**Fig. 20-12.** Passband echo canceler for a voiceband data modem with complex cancellation.

whether the phase error  $\theta_k - \hat{\theta}_k$  is positive or negative by examining the imaginary-part of the rotated error. If this imaginary-part is positive, the error is reduced by making the estimated phase  $\hat{\theta}$  larger.

A SG PLL algorithm for adjustment of the phase follows from the derivative in Exercise 20-5,

$$\hat{\theta}_k = \hat{\theta}_{k-1} + \beta \cdot \text{Im}\{E_k e^{-j\hat{\theta}} E_k \mathbf{c}_k^* \tilde{\mathbf{a}}_k^*\} . \tag{20.55}$$

**Exercise 20-6.** Show that if the echo canceler transversal filter has converged and there is no far-end signal or noise,

$$E[\text{Im}\{E_k e^{-j\hat{\theta}} E_k \mathbf{c}_k^* \tilde{\mathbf{a}}_k^*\}] = \sigma_a^2 \|\mathbf{c}_k\|^2 \cdot \sin(\theta_k - \hat{\theta}_k) . \tag{20.56}$$

Thus, the SG PLL algorithm is first order with a sinusoidal phase detector.

## 20.6. FURTHER READING

Several tutorial papers are available on general echo cancellation topics [13][14][15]. The digital subscriber loop echo canceler application is summarized in [3], with more details given in [10][4][16]. For the voiceband data modem application, the early papers by Weinstein are recommended [7] as well as the more recent article by Werner which proposes the passband transversal filter approach [8].

There are numerous techniques for speeding up adaptation of the echo canceler using more sophisticated adaptation algorithm. For some references, see Section 9.6. In data echo cancellation in particular, a significant factor slowing adaptation is the far-end data signal. This suggests another means of speeding adaptation, in which the data signal is adaptively removed from the cancellation error in a decision-directed fashion [17] in an approach called an *adaptive reference canceler*.

Another possibility is to use the least-square algorithm mentioned in Section 9.2. The data symbols can be chosen during a training period to assist in the canceler adaptation. In this case, the transmitted signal algebraic properties become much more important than the stochastic properties which we have emphasized in our convergence results. It has been shown that the

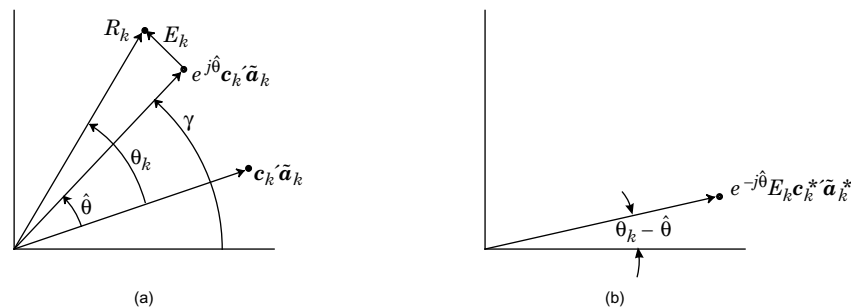


**Fig. 20-13.** Interpretation of far-end echo canceler phase detector. a. Transversal filter and echo channel output. b. Rotated so that the echo replica is on the real-axis.

mean values of the filter coefficients of a canceler based on least-squares can converge in  $N$  data symbols for an  $N$ -tap canceler [18]. Furthermore, it has been shown that the least-squares algorithm can be virtually as simple as the stochastic gradient algorithm for a reference signal which is chosen to be a pseudo-random sequence [19]. This sequence is also particularly simple to generate during a training period.

The implementation of a data echo canceler in monolithic form represents special challenges because of the high accuracy required. This is discussed in more depth in [10][4].

Some older work in speech cancelers and some more recent work in data cancelers has extended the adaptive echo canceler technique to nonlinear echo generation phenomena [20][21]. In data transmission, the objectives for degree of cancellation are sufficiently ambitious that nonlinear echo generation phenomena are of importance [10][21][4].

## Appendix 20-A. Real-Error Canceler Convergence

---

In this appendix we analyze the convergence of the real error canceler for a passband channel and passband transversal filter. In general we will find that we must make stronger assumptions for this case to get simple results than we made in the complex error case. Specifically, we often have to assume independence of random variables whereas in the complex error case uncorrelated random variables will suffice.

We can find the minimum MSE solution for the real error canceler most easily by using the gradient formula derived in Exercise 20-3,

$$\nabla_c(\text{Re}\{E_k\}) = -2\text{Re}\{E_k\} \tilde{\mathbf{a}}_k^* \quad . \quad (20.57)$$

Equating the expected value with the zero vector will give us the optimum coefficient vector. The evaluation of this expected value is aided by the following result:

**Exercise 20-7.** Given a sequence of transmitted rotated data symbol which are mutually independent, and for which the real and imaginary parts are zero-mean, identically distributed, and independent, show that

$$E[\tilde{\mathbf{a}}_k \tilde{\mathbf{a}}_k'] = \mathbf{0} \quad . \quad (20.58)$$

Similarly, for the same assumptions on the uncancelable error  $V_k$ , show that

$$E[V_k^2] = 0 \quad . \quad (20.59)$$

Lest this latter result seem strange, remember that  $V_k$  is complex valued, and hence its variance is  $E[|V_k|^2]$ , not  $E[V_k^2]$ .

Using this result and taking the expected value of (20.57), we get immediately

$$\Phi(\tilde{\mathbf{h}} - \mathbf{c}) + \mathbf{p} + \mathbf{q} = \mathbf{0} \quad , \quad (20.60)$$

where  $\Phi$  and  $\mathbf{p}$  are defined as before and

$$\mathbf{q} = E[V_k^* \tilde{\mathbf{a}}_k^*] . \quad (20.61)$$

It follows that the optimum coefficient vector is

$$\mathbf{c}_{\text{opt}} = \tilde{\mathbf{h}} + \Phi^{-1}(\mathbf{p} + \mathbf{q}) , \quad (20.62)$$

which is almost the same as for the complex error case with the addition of the  $\mathbf{q}$  term. In fact, for the important case where the uncancelable error is independent of the transmitted data symbols and both are zero-mean, (20.62) reduces to  $\mathbf{c}_{\text{opt}} = \tilde{\mathbf{h}}$  and the solution is the same as for the complex error case.

The real error SG algorithm is given by (20.36). We can easily develop a stochastic difference equation governing the trajectory of the coefficient vector error.

**Exercise 20-8.** In analogy to Exercise 20-4, show that for the real error algorithm we get a slightly more complicated result

$$\mathbf{q}_k = \Gamma_k \mathbf{q}_{k-1} - \Lambda_k \mathbf{q}_{k-1}^* + \beta \text{Re}\{D_k\} \tilde{\mathbf{a}}_k^* \quad (20.63)$$

where the stochastic matrices are

$$\Gamma_k = \mathbf{I} - \frac{1}{2} \beta \tilde{\mathbf{a}}_k^* \tilde{\mathbf{a}}_k, \quad \Lambda_k = \frac{1}{2} \beta \tilde{\mathbf{a}}_k^* \tilde{\mathbf{a}}_k^{*'} . \quad (20.64)$$

Fortunately, under reasonable assumptions the three terms in (20.63) are independent. First, from the orthogonality principle that the real error for the minimum MSE canceler  $\text{Re}\{D_k\}$  is uncorrelated with the sequence of transmitted data symbols,

$$E[\text{Re}\{D_k\} \tilde{\mathbf{a}}_k^*] = \mathbf{0} . \quad (20.65)$$

If we further assume that  $D_k$  is independent of the transmitted data symbols, and zero-mean, then the expected value of any cross terms between  $\text{Re}\{D_k\}$  and  $\Gamma_k$  or  $\Lambda_k$  will be zero. Further,  $\Gamma_k$  and  $\Lambda_k$  are themselves uncorrelated.

**Exercise 20-9.** Using the results of Exercise 20-7, show that

$$E[\Gamma_k \Lambda_k^*] = \mathbf{0} . \quad (20.66)$$

Now we are prepared to determine the expected value of  $\|\mathbf{q}_k\|^2$ , using in part the results of Appendix 9-A. From that appendix (recall that the definition of  $\Gamma_k$  is slightly different here),

$$E[\Gamma_k^* \Gamma_k] = (1 - \beta \sigma_a^2 + \frac{1}{4} \beta^2 (\eta_\alpha + (N-1) \sigma_a^4)) \cdot \mathbf{I}, \quad \eta_\alpha = E[|a_k|^4] . \quad (20.67)$$

By a similar computation, we can find the second term.

**Exercise 20-10.** Show that approximately

$$E[\Lambda_k^{*'} \Lambda_k] = \frac{1}{4} \beta^2 \sigma_a^4 \cdot \mathbf{I} . \quad (20.68)$$

Finally, the expected norm-squared of (20.63) becomes the expected norm-squared of three terms,

$$E[\|\Gamma_k \mathbf{q}_{k-1}\|^2] = \mathbf{q}_{k-1}^{*'} E[\Gamma_k^* \Gamma_k] \mathbf{q}_{k-1} = (1 - \beta \sigma_a^2 + \frac{1}{4} \beta^2 (\eta_\alpha + (N-1) \sigma_a^4)) \|\mathbf{q}_{k-1}\|^2 , \quad (20.69)$$

$$E[\|\Lambda_k \mathbf{q}_{k-1}\|] = \mathbf{q}'_{k-1} E[\Lambda_k^* \Lambda_k] \mathbf{q}_{k-1} = \frac{1}{4} \beta^2 (\eta_\alpha + (N-1)\sigma_\alpha^4) \|\mathbf{q}_{k-1}\|^2, \quad (20.70)$$

$$E[\|\beta \operatorname{Re}\{D_k\} \tilde{\mathbf{a}}_k^*\|^2] = \beta^2 E[(\operatorname{Re}\{D_k\})^2] \|\tilde{\mathbf{a}}_k\|^2 = N\sigma_\alpha^2 \beta^2 E[(\operatorname{Re}\{D_k\})^2]. \quad (20.71)$$

Evaluation of this expression is aided by the following result.

**Exercise 20-11.**

- (a) Assume that the uncancelable error  $D_k$  consists of a filtered far-end data signal plus an additive noise. Further make the usual independence and white-noise assumptions on these two components and show that

$$E[D_k^2] = E[(D_k^*)^2] = 0. \quad (20.72)$$

- (b) Show that

$$E[(\operatorname{Re}\{D_k\})^2] = \frac{1}{2} E[|D_k|^2] = \frac{1}{2} \xi_{\min}. \quad (20.73)$$

In other words, the real and imaginary parts of  $E[|D_k|^2]$  are equal.

These results give the following difference equation for the norm-squared error vector,

$$E[\|\mathbf{q}_k\|^2] = \gamma E[\|\mathbf{q}_{k-1}\|^2] + \frac{1}{2} N\sigma_\alpha^2 \beta^2 \xi_{\min}, \quad (20.74)$$

$$\gamma = 1 - \beta\sigma_\alpha^2 + \frac{1}{2} \beta^2 (\eta_\alpha + (N-1)\sigma_\alpha^4). \quad (20.75)$$

Now we are in a position to compare the real error and complex error cancelers. First looking at the asymptotic MSE, the complex error case is given by (20.49), whereas from (20.74)

$$E[\|\mathbf{q}_k\|^2] \rightarrow \frac{N\beta}{2 - N\beta\sigma_\alpha^2} \cdot \xi_{\min}, \quad (20.76)$$

which is the same as (20.49). Similarly, calculating an approximate time constant  $\tau$  from (20.75) as  $\gamma^\tau = 1/e$ , we get for small step-size

$$\tau \approx \frac{1}{\beta\sigma_\alpha^2}, \quad (20.77)$$

which is twice as long as for the complex error canceler (20.46).

## Problems

**Problem 20-1.** Consider using echo cancellation for a digital subscriber loop with AMI line coding (Section 19.1). What options are there for realization of the line coder, and where would it be most reasonable to connect the echo canceler input?

**Problem 20-2.** Consider a V.32 voiceband data modem with the following parameters: baud rate 2400 Hz, carrier frequency 1800 Hz, passband channel covering the band from 300 to 3000 Hz. Further assume that the echo response has a duration of 32 baud intervals.

- Assuming the receive signal is sampled at a rate equal to an integer multiple of the baud rate, what is the most reasonable sampling rate? Discuss the considerations in the choice of this rate.
- For this sampling rate, compare the multiplication rate for two cancelers, one connected to the sampled transmitted waveform and the other to the transmitted data symbols.

**Problem 20-3.** For a passband echo canceler, it is possible to put a demodulator in the receiver prior to cancellation of the echo.

- Show two alternative configurations, one using a phase splitter and the other a lowpass filter. Develop an equivalent echo channel model analogous to Fig. 20-7.
- Is it possible or reasonable to consider a real-error canceler for this configuration?
- Describe the echo canceler required for this configuration.
- How will the adaptation rate of this configuration compare to the configurations considered in Section 20.3?
- Discuss the advantages and disadvantages of this configuration.

**Problem 20-4.** Assuming the echo response extends for  $N$  baud intervals and  $R$  interleaved cancelers, compare the complexity as measured in equivalent real-valued multiplication rates for all combinations of a baseband and passband transversal filter with a real-error and complex-error canceler. Which configurations are more attractive in accordance with this complexity metric?

**Problem 20-5.** How would you modify Fig. 20-10 to use a complex-error canceler? Show that only one phase splitter is required, at the expense of a second lowpass filter.

**Problem 20-6.** Determine the MSE solution for the complex-error canceler with baseband transversal filter, and find the optimal coefficient vector. *Hint:* Show that minimizing  $E[|E_k|^2]$  is equivalent to minimizing  $E[|e^{-j2\pi f_c(k+l/R)T} E_k|^2]$ , and then minimize the latter quantity.

**Problem 20-7.** For a passband echo channel, we can use a baseband echo canceler followed by modulator, or a modulator (rotator) followed by passband echo canceler. Give a convincing argument that the convergence rate and asymptotic MSE of the baseband echo canceler is the same as the convergence rate and MSE of the passband echo canceler.

**Problem 20-8.**

- The PLL algorithm of Exercise 20-6 will have a tracking capability somewhat dependent on the echo impulse response. Explain.
- How would you fix this problem?

**Problem 20-9.**

- Show that

$$\frac{\partial(\operatorname{Re}\{E_k\})^2}{\partial\hat{\theta}} = -2\operatorname{Re}\{E_k\}\operatorname{Im}\{e^{-j\hat{\theta}} \mathbf{c}_k^* \tilde{\mathbf{a}}_k^*\}. \quad (20.78)$$

- Use this result to develop a first-order PLL algorithm that uses only the real-error. Interpret this algorithm graphically.

- (c) Find the expected value of the phase correction term.

## References

---

1. B. Aschrafi, P. Meschkat, and K. Szechenyi, "Field Trial of a Comparison of Time Separation, Echo Cancellation, and Four-Wire Digital Subscriber Loops," Proceedings of the Int. Symp. on Subscriber Loops and Services, (Sep. 1982).
2. J-O. Andersson, B. Carlquist, A. Bauer, and I. Dahlqvist, "An LSI Implementation of an ISDN Echo Canceller: Design and Network Aspects," *IEEE Journal on Selected Areas in Communications*, November 1986.
3. D. G. Messerschmitt, "Design Issues for the ISDN U-Interface Transceiver," *IEEE Jour. on Special Areas in Communications*, (Nov. 1986).
4. O. Agazzi, D. A. Hodges, and D. G. Messerschmitt, "Large-Scale Integration of Hybrid-Method Digital Subscriber Loops," *IEEE Trans. on Communications*, Vol. COM-30, p. 2095 (Sep. 1982).
5. J. Tzeng, D. Hodges, and D. G. Messerschmitt, "Baud Rate Timing Recovery in Digital Subscriber Loops," *IEEE Int. Conf. on Communications*, (June 1985).
6. K. H. Mueller and M. Muller, "Timing Recovery in Digital Synchronous Data Receivers," *IEEE Trans. on Communications*, Vol. COM-24, pp. 516-531 (May 1976).
7. S. B. Weinstein, "A Passband Data-Driven Echo Canceller for Full-Duplex Transmission on Two-Wire Circuits," *IEEE Trans. on Communications*, (July 1977).
8. J. J. Werner, "An Echo-Cancellation-Based 4800 Bit/s Full-Duplex DDD Modem," *IEEE Journal on Selected Areas in Communications*, Vol. SAC-2 (5), (Sep. 1984).
9. B. Widrow, J. McCool, M. Larimore, and C. Johnson, Jr., "Stationary and Non-Stationary Learning Characteristics of the LMS Adaptive Filter," *Proc. IEEE*, Vol. 64 (8), pp. 1151-1162 (Aug. 1976).
10. N. A. M. Verhoeckx, H. C. Van Den Elzen, F. A. M. Sniijders, and P. J. Van Gerwen, "Digital Echo Cancellation for Baseband Data Transmission," *IEEE Trans. on ASSP*, Vol. ASP-26 (6), (Dec. 1979).
11. D. L. Duttweiler, "A Twelve-Channel Digital Echo Canceller," *IEEE Trans. on Communications*, pp. 647-653 (May 1978).
12. M. L. Honig and D. G. Messerschmitt, *Adaptive Filters: Structures, Algorithms, and Applications*, Kluwer Academic Publishers, Boston (1984).
13. M. Sondhi and D. A. Berkley, "Silencing Echos on the Telephone Network," *IEEE Proceedings*, Vol. 8, (Aug. 1980).
14. D. G. Messerschmitt, "Echo Cancellation in Speech and Data Transmission," *IEEE Jour. on Selected Areas in Communications*, Vol. SAC-2 (2), p. 283 (March 1984).
15. D. G. Messerschmitt, "Echo Cancellation in Speech and Data Transmission," pp. 182 in *Advanced Digital Communications Systems and Signal Processing Techniques*, ed. K. Feher, Prentice-Hall, Englewood Cliffs, N.J. (1987).

16. O. Agazzi, D. G. Messerschmitt, and D. A. Hodges, "Nonlinear Echo Cancellation of Data Signals," *IEEE Trans. on Communications*, Vol. COM-30, p. 2421 (Nov. 1982).
17. D. D. Falconer, "Adaptive Reference Echo Cancellation," *IEEE Trans. on Communications*, Vol. COM-30 (9), (Sept. 1982).
18. T. L. Lim and M. S. Mueller, "Rapid Equalizer Start-Up Using Least Squares Algorithms," *Proc. International Conference on Communications*, (1980).
19. J. Salz, "On the Start-Up Problem in Digital Echo Cancellers," *Bell System Technical Journal*, Vol. 60 (10), pp. 2345-2358 (July-Aug., 1983).
20. E. J. Thomas, "Some considerations on the application of the Volterra representation of nonlinear networks to adaptive echo cancellers," *Bell System Technical Journal*, Vol. 50 (8), pp. 2797-2805 (Oct. 1971).
21. N. Holte and S. Stueflotten, "A New Digital Echo Canceler for Two-Wire Subscriber Lines," *IEEE Trans. on Communications*, Vol. COM-29 (11), pp. 1573-1581 (Nov. 1981).

